

EFFECTS OF Sb, In, AND Sn DOPING
ON OPTICAL PROPERTIES OF SnO_2

C. J. GIBSON

M. Eng.

THE EFFECTS OF Sb, In, AND Sn DOPING
ON THE
OPTICAL PROPERTIES OF TIN DIOXIDE

by

CAREY JAMES GIBSON , B.Sc.

PART A : McMASTER (ON-CAMPUS) PROJECT *

A Report

Submitted to the School of Graduate Studies
in Partial Fulfilment of the Requirements
for the Degree
Master of Engineering

September 1976

* One of two project reports: The other is designated

PART B : McMASTER (OFF-CAMPUS) PROJECT

MASTER OF ENGINEERING (1976)
Department of Engineering Physics

McMASTER UNIVERSITY
Hamilton, Ontario

TITLE: THE EFFECTS OF Sb, In, AND Sn DOPING ON THE OPTICAL PROPERTIES
OF TIN DIOXIDE

AUTHOR: CAREY JAMES GIBSON, B. Sc. (Dalhousie University)

SUPERVISOR: Dr. J. P. Marton

NUMBER OF PAGES: vii, 47

ABSTRACT

This study was focused on the absorption spectra of tin dioxide thin films on optical quartz substrates. The films were doped with antimony from zero to ten percent, indium from zero to ten percent, and intrinsically, by heating undoped samples in vacuum and air. The surface resistances were also measured.

The results for antimony doping show that the energy required for electron transitions from valence to conduction bands, the associated phonon energies, and the optical absorption by free carriers all increase while resistance decreases with increased doping. These results are consistent with antimony acting as a donor in SnO_2 and elevating the Fermi level, which is in the conduction band for the undoped material, to a higher level, thus increasing the free carrier concentration. The results possibly also indicate a strain on the lattice caused by doping.

The results for indium doping show a similar increase in energies along with a decrease in optical absorption by free carriers and an increase in resistance with increased doping. The indium acts as an acceptor and, in so doing, causes the Fermi level to drop into the valence band, at the doping levels used in this study. This is probably due to the formation of an acceptor band above or overlapping the valence band and resulting in a reduction of the free carrier concentration. The increase in phonon energy indicates that the doping

imposes a strain on the lattice.

Heating undoped films in vacuum appears to drive off oxygen resulting in reduced resistance and therefore higher free carrier concentration due to lattice defect doping, and reduced valence to conduction band transition energy possibly due to the formation of a conduction band in the forbidden band-gap. The changes were reversible by re-heating in air.

ACKNOWLEDGEMENTS

The author would like to express his thanks to Dr. J. P. Marton of McMaster University for his supervision and assistance in this project, and to Dr. B. Jordan of McMaster University for his help with the experimental part of this work.

TABLE OF CONTENTS

	<u>PAGE</u>
ABSTRACT	iii
ACKNOWLEDGEMENTS	v
LIST OF ILLUSTRATIONS	vii
CHAPTER 1: INTRODUCTION	1
CHAPTER 2: THEORY	
2.1 General Properties	5
2.2 Absorption Edge Properties	9
2.3 Doping, Impurity, and Defect Properties	12
CHAPTER 3: EXPERIMENTAL PROCEDURE	
3.1 Sample Preparation	17
3.2 Resistance Measurements	18
3.3 Optical Measurements	18
CHAPTER 4: RESULTS	
4.1 Preparation Effects	20
4.2 Antimony Doping	25
4.3 Indium Doping	31
4.4 Self-Doping	37
CHAPTER 5: CONCLUSIONS	43
REFERENCES	46

LIST OF ILLUSTRATIONS

<u>FIGURE</u>		<u>PAGE</u>
1	Band Structure of SnO_2 by T. Arai ⁽¹⁾ . . .	3
2	Spectral Response of SnO_2 Thin Film (T.F.10) . .	22
3	Absorption Coefficient Times Film Thickness for SnO_2 Thin Film (T.F.12d) . . .	24
4	Absorption Spectra of 10 % Sb Doped SnO_2 (T.F.16) versus Undoped SnO_2 (T.F.12a). . .	26
5	Absorption Edge Energy of Sb Doped SnO_2 . . .	27
6	Surface Resistance per cm^2 of Sb Doped SnO_2 . .	29
7	Phonon Energy for Sb and In Doped SnO_2 . . .	30
8	Absorption Spectra of 5 % In Doped SnO_2 (T.F.24) versus Undoped SnO_2 (T.F.12a). . .	33
9	Absorption Edge Energy of In Doped SnO_2 . . .	34
10	Surface Resistance per cm^2 of In Doped SnO_2 . .	36
11	Consecutive Absorption Spectra of Treated SnO_2 (T.F.12)	38
12	Measured Absorption Edge Energies for Treated SnO_2 (T.F.12)	39
13	Surface Resistance per cm^2 of Treated SnO_2 (T.F.12) .	40

CHAPTER 1

INTRODUCTION

Tin dioxide is an unusual material in that it is, generally speaking, a conductor that is transparent over the visible spectrum. In its purest form, SnO_2 is insulating,⁽¹⁾ but under usual preparation conditions, the defect structure of the material results in an n-type intrinsic semiconductor. With proper doping, SnO_2 properties can approach those of either a metal or a good insulator, as will be discussed later in this report. The transparency and conduction exhibited by SnO_2 results in practical applications as a conductive coating on such things as lenses and optical cells. Also, films of this material are very robust and do not oxidize making them ideal as conductors for resistive and heating elements. The possibility exists that SnO_2 may be useful as a high temperature semiconductor for electronics applications.

Serious studies of the properties of tin dioxide started in 1954 with a report published by R. Aitchison⁽²⁾ in which the optical and electrical properties of doped and pure SnO_2 were observed. Since that time many others^(2,4,5,6,8,11,12) have looked at these properties under different conditions. Others have observed the physical characteristics of the films.⁽³⁾ A theoretical band-scheme for SnO_2 has been developed by T. Arai⁽¹⁾ and

mathematics relating absorption to theoretical structure have been formulated. (9,10) A comprehensive review of the whole tin oxide field has recently been prepared. (4) The theoretical band-gap diagram for SnO_2 as developed by T. Arai is shown in Figure 1. (1)

There is some variation in the values of the band-gap energy obtained from absorption spectra. T. Arai has found values for E_g ranging from $3.71 \pm .03$ eV to $3.82 \pm .03$ eV for non-conducting and conducting SnO_2 respectively, the difference being due to the filling up of the conduction band by free carriers. W. Spence has obtained values of approximately 3.7 eV for the same absorption edge with direct band-gap transitions indicated at 4.3 eV and indirect transitions indicated at 2.7 eV. (7) (These last two values were calculated using the squares and square roots of the absorption coefficients respectively.) Also observed was an impurity peak at 3.36 eV which was attributed to either an impurity or an exciton.

This report looks at the theoretical and experimental response of thin films of SnO_2 to impurity doping with antimony and indium which are group V and group III respectively in the periodic table, on either side of tin; and at the theoretical and experimental response to intrinsic doping which was achieved by driving off oxygen in a vacuum furnace and by oxidizing the sample. The surface resistivity of the samples was also examined.

The samples were prepared by spraying a mixture of chlorides of tin and proportioned amounts of antimony or indium up to ten per cent, along with hydrochloric acid and water onto quartz sub-

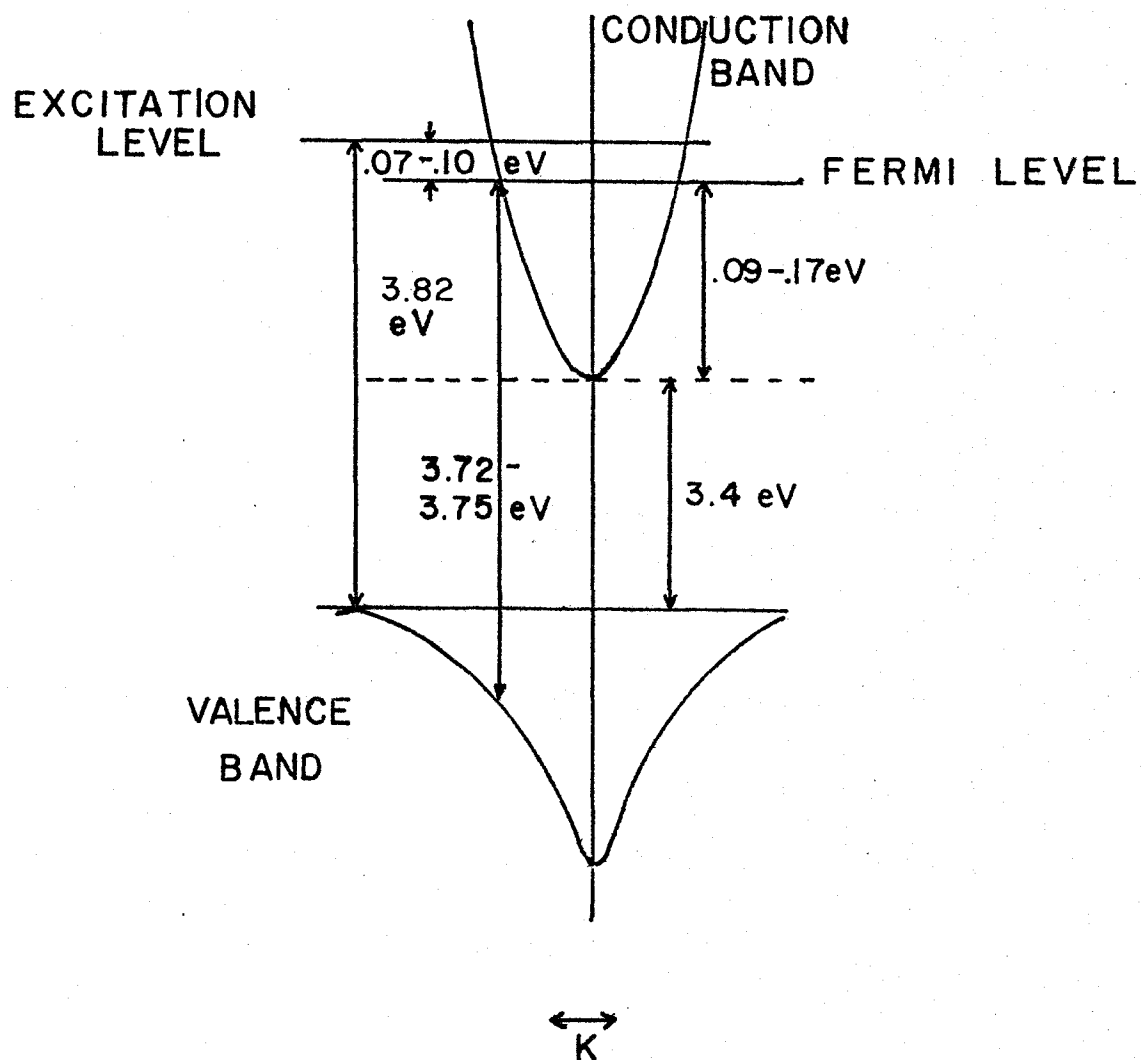


Figure 1.

Band Structure of SnO_2 by T. Arai (1)

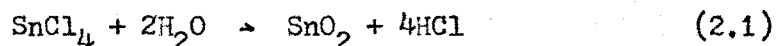
strates at high temperatures where the reaction of the chlorides and water produced the desired oxide. The samples were then studied by measuring the optical transmission and reflection covering the visible spectrum (2600 - 220 nm.) as well as measuring the resistivity per square of surface. The intrinsic doping samples were then heat-treated in either air or vacuum and re-measured. From the transmission and reflection spectra absorption coefficients were used to determine the band-gap energies of the samples.

CHAPTER 2

THEORY OF SnO_2 THIN FILMS

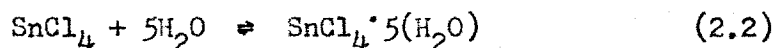
2.1 General properties

The thin films of SnO_2 used in this study were prepared from the reaction



which proceeds quickly at temperatures above 500 degrees centigrade.⁽²⁾

At temperatures significantly below this, these compounds may also react according to the formula



The hydrated stannic chloride forms a precipitate in water. This precludes the vapour method of film formation normally used where the stannic chloride and water react on the substrate surface at high temperature. Adding a large proportion of hydrochloric acid to this reaction mixture prevents the formation of any significant amount of hydrated stannic chloride at low temperatures, and at high temperatures probably has the effect of slowing down the reaction rate, thus resulting in a more uniform film structure. It may, however, have the effect of increasing the defect level in the film composition by adding oxygen ion deficiencies and chlorine ions. These impurities will be discussed later.

The upper temperature boundaries for both the formation and use of tin dioxide films are partially dependant on the substrate used. On ordinary glass the films show irreversible changes above approximately 550 degrees C.⁽³⁾ These changes are mainly a result of the formation of larger, irregular crystals on the film surface, which causes a higher resistance in the film. This is probably caused by reactions with sodium or potassium silicates in the glass, which softens at about this temperature. On quartz substrates some structural changes are seen above 650 to 700 degrees C. or higher.⁽³⁾ These changes are generally speaking an increase in grain size of the film without breaking the cohesion of the particles. As no chemical reaction takes place, there is no large change in resistance. When heated above 850 to 900 degrees C. the films on quartz tend to break up. On ceramic substrates there is some evidence that stable films can be formed at temperatures of 1050 degrees C. or above.

Tin dioxide films are usually poly-crystalline in structure, although epitaxial thin films can be grown on appropriate substrates. The crystals have a tetragonal rutile structure with a unit cell containing two tin and four oxygen atoms in a 6 : 3 structural coordination. Each tin atom is placed at the center of six oxygen atoms, the sites of which approximately form the corners of a regular octahedron, while three tin atoms are more or less equidistant from each other around each oxygen atom.⁽⁴⁾

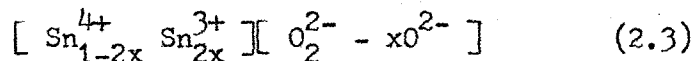
The properties of bulk tin dioxide in thin films differ from those of the surface layer. Typically, the bulk resistance may

be of the order of one Ohm-cm. while the surface resistivity may be 10^4 to 10^5 Ohm-cm., the high resistivity possibly being due to iron or aluminum doping of the surface by ceramics or other materials being used. Adherent, uniform layers are generally transparent, while thicker films usually have a white, scattering appearance due to the formation of microscopic tin dioxide particles on the surface.⁽²⁾ These particles may also contribute to higher surface resistance by providing a non-continuous surface contact.

The resistivity of tin dioxide is largely determined by the concentration and scattering of free carriers. The majority carriers are electrons, causing the material to act as an n-type semiconductor under most circumstances. The free carriers are largely scattered by ionized centers. Thus, impurity scattering of free carriers is the predominant process in the conduction mechanism. The properties of the free carriers strongly influence the optical properties in the near infra-red spectrum.⁽⁵⁾ The major native ionized defect in tin dioxide appears to be a doubly ionizable oxygen vacancy. Deposited SnO_2 films generally depart appreciably from stoichiometric proportions with resistance measurements showing an excess of tin. There are a number of possible types of defect structure, due to the rutile configuration of the crystals. The relatively low concentration of free carriers, about 7 to $17 \times 10^{18} \text{ cm.}^{-3}$ in conducting SnO_2 ,⁽¹⁾ results in a plasma frequency which lies in the near infra-red region. The higher carrier concentration of metals places their plasma frequencies in the ultra-violet region. Thus, in spite of its metallic conduction, SnO_2 is transparent in the visible spectrum with the

position of the absorption threshold due to free carriers in the infra-red portion of the spectrum. (6)

The free carrier concentration has an additional effect attributed to it. This is the elevation of the absorption edge, representing the band-gap energy, by an activation energy of approximately 0.1 electron volts for conducting SnO_2 over that for non-conducting SnO_2 as shown in figure 1. (1) The theoretical explanation for this effect is that the free carriers fill up the bottom of the conduction band and thus new carriers elevated to the conduction band must have an energy that is increased by the excitation energy of this filled up region. This combination of conduction band and excitation energy is caused by overlapping with impurity levels. SnO_2 thin films are generally conductive upon fabrication, however they can be made non-conductive by heating in air (annealing). This is probably due to the removal of oxygen defects by oxidation of the film. Air annealing causes the film to become a highly n-type semiconductor. Vacuum annealing, on the other hand, causes the film to be reduced. If the film is sufficiently reduced, both n-type and p-type semiconductor behavior is observed. (7) The reduced film has the stoichiometric chemical formula (2) :



Upon fabrication, some oxygen vacancies may be occupied by chlorine ions. This will be discussed further in section 2.3.

2.2 Absorption Edge Properties

The optical absorption spectrum of SnO_2 contains much information about the material. The properties of the infra-red and visible spectra have been mentioned briefly in the previous section and this section will deal mainly with the absorption edge of SnO_2 which occurs in the far visible to near ultra-violet region of the spectrum. Below this edge, SnO_2 is basically transmitting except for a few absorbing bands in the infra-red spectrum mainly attributable to impurity structures. Above this edge, SnO_2 is almost totally absorbing.

The absorption edge begins at the point where the photon energy equals the band-gap energy,

$$h\nu = E_g. \quad (2.4)$$

At this energy, photons excite electrons from the valence band to the conduction band. Direct band-gap transitions result in intense absorption, while indirect transitions, requiring phonon assistance, are less intense.

The absorption coefficient K , for direct transitions, has the theoretical value

$$K = A (h\nu - E_g)^{\frac{1}{2}} \quad (2.5)$$

where h and E_g are the photon and band-gap energies respectively and A has the value⁽⁸⁾

$$A = 3.38 \times 10^7 \text{ m}^{-1} \left(\frac{m_e}{m_0} \right)^{\frac{1}{2}} \left(\frac{E_g}{h\nu} \right). \quad (2.6)$$

However, A varies slowly and can be thought of as constant over a narrow range. This formula for K over-simplifies the case for direct transitions in that it predicts that K will fall off to zero for

$h\nu < E_g$. This does not happen in general because of the impurity and defect structure of the material in question. This will be discussed further in section 2.3. Also, electron-hole Colomb interactions tend to square off the edge and give larger absorption, but this effect is screened by high free carrier concentrations or defect and impurity levels.⁽⁸⁾

The discussion of tin dioxide is more complicated than that given above, however, because SnO_2 undergoes an indirect (phonon assisted) transition. For indirect transitions assisted by a single phonon, the formula for the absorption coefficient takes the form

$$K \propto \frac{(h\nu + E_p - E_g)^2}{\exp(E_p/kT) - 1} + \frac{(h\nu - E_p - E_g)^2}{1 - \exp(-E_p/kT)} \quad (2.7)$$

where E_p is the phonon energy.⁽⁸⁾ For forbidden transitions,

$$K \propto (h\nu \pm E_p - E_g)^3. \quad (2.8)$$

Thus, for a single phonon assisted indirect transition, a graph of $K^{\frac{1}{2}}$ versus $h\nu$ should have two linear regions extrapolating to $E_g + E_p$ and $E_g - E_p$. Unfortunately, this is also an over-simplification in the case of tin dioxide. SnO_2 has altogether not one but eleven optical phonon modes and possibly many acoustic modes which may participate in indirect transitions, thus complicating the picture further.⁽⁷⁾ However, it is generally accepted that the single phonon formulation, as represented in equation 2.7 is a good approximation of the actual case.

Absorption by free carriers in general follows the formula

$$K \propto \lambda^p \quad (2.9)$$

where p is a factor dependant on the charge scattering process. Common values of p are $p = 2$ for acoustic mode scattering, $p = 2.5$ for optical phonon scattering, and $p > 3$ for ionized defect or impurity scattering.⁽⁴⁾ The major scattering in tin dioxide is performed by optical phonons. An additional complication affecting this edge measurement is the poly-crystalline nature of the films which reduces the sharpness of the edge.

The generally (but not universally) accepted method for analysing the absorption edge is to plot K and/or $K^{\frac{1}{2}}$ versus $h\nu$ which results (hopefully) in two linear regions which are extrapolated to find the values of $E_g + E_p$ and $E_g - E_p$ at $K = 0$. The highest value of E_p for pure SnO_2 is 0.08 eV or less, which represents the highest optical lattice mode.⁽⁴⁾

The absorption coefficient is found experimentally from the transmission and reflection spectra of the sample. The formula relating these values is

$$T = \frac{(1 - r^2) \exp(-Kd)}{\exp(-2Kd) - r^2} \quad (2.10)$$

where T is transmission, r is reflection, K is the absorption coefficient, and d is the film thickness, all at a single value of incident photon energy.⁽⁹⁾ For cases where r is negligible, equation 2.10 can be easily simplified to

$$Kd = -\log_e(T) \quad (2.11)$$

However, for the case where this simplification cannot be made, A. Kahan⁽¹⁰⁾ has re-arranged the equation into a solvable form as follows:

$$K_d = \frac{1}{2} \log_e \left[\frac{A + (A^2 + 4T^2)^{\frac{1}{2}}}{2T} \right] \quad (2.12)$$

where

$$A = T^2 - (r - 1)^2. \quad (2.13)$$

The same paper also defines an extinction coefficient k as being

$$k = \frac{\lambda}{4\pi} K. \quad (2.14)$$

2.3 Doping, Impurity, and Defect Properties

This section deals with the theoretical aspects of introducing foreign ions or defects into the structure of tin dioxide. Four separate effects are of importance in this study. They are the introduction of defects into the structure in the form of oxygen deficiencies, impurity doping predominately by chlorine, intentional doping with antimony, and intentional doping with indium.

Of the above effects, oxygen deficiencies, antimony ions, and chlorine ions are all reducing agents which increase the carrier concentration, and indium ions tend to oxidize SnO_2 reducing the carrier concentration. To this point in the literature on the subject, much more theoretical interest has been shown in the introduction of reducing agents into SnO_2 films than has been shown in doping with oxidizing agents, which have been practically ignored. Thus the effect of doping with materials such as indium has not been satisfactorily explained to date.

The mechanism and effects of oxygen deficiencies have been partially explained in section 2.1. Basically, the tin ion prefers to

have a 4^+ charge and the oxygen ion prefers a 2^- charge. A missing oxygen ion means that the tin ion may only have a net 2^+ charge and the two loosely bound electrons of the tin ion are added to the conduction band. As already explained, this results in reduced resistivity and an increased band-gap energy due to the filling up of the conduction band. The degree of oxygen deficiency has an effect on the stability of the film properties. This results from the oxidation of partially reduced films in air, which proceeds very slowly at room temperature but more quickly at temperatures above 500°C .

Nagasawa and Shionoya⁽¹²⁾ have shown in their studies that oxidation and reduction of SnO_2 results in large changes in the lower (infra-red) absorption edge of the transparent band. Their results showed the lower edge occurring at greater than seven microns wavelength for the oxidized material, while the lower edge occurred at under two microns for the reduced material.

Chlorine atoms are generally the main impurity centers in undoped SnO_2 films prepared by the reaction of tin chloride. These atoms may be included either interstitially or substitutionally.⁽⁴⁾ In the substitutional case, the chlorine atom replaces an oxygen atom. In terms of valence, this is like a deficiency of half an oxygen ion, and a corresponding increase in conductivity is seen similar to that with the oxygen deficiency. This is not the total story, however, as the properties of the chlorine substitution are not identical to the properties of an oxygen vacancy. Replacing the oxygen ion with a chlorine ion leads to the formation of donor levels close to the conduction band. If the impurities are present in

sufficient concentration (greater than 10^{19} per cubic centimeter), the impurity and conduction bands will blend together. This results in one conduction band, as with pure SnO_2 , but at a higher level (due to the filling up effect).⁽¹¹⁾ Chlorine ions may affect the stability of the film. When heated, chlorine ions may be replaced with oxygen ions resulting in irreversible changes in the film properties. Trace doping (contamination) with such materials as iron and aluminum and sometimes silicon during preparation has no noticeable effect on the bulk properties of the material but, as already noted, affects the surface resistivity.

Antimony, when included in the n-type semiconducting SnO_2 , acts as a donor. The addition of the Sb^{5+} ion is like reducing a Sn^{4+} ion to Sn^{3+} and may do just that.⁽²⁾ Antimony increases the number of defect centers. The antimony ions substitute for tin ions in the crystal structure which then has the chemical structure

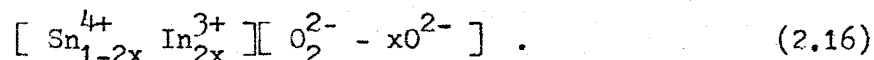


The occurrence of defect-related absorption is noticed as the number of defect centers reaches about ten percent, at which point the effective diameters of the impurity centers are twice the normal lattice spacing.⁽²⁾ Antimony doped films show considerable absorption in the infra-red spectrum resulting in a blueish color.⁽¹¹⁾

A. Rohatgi, et al.⁽¹³⁾ have looked at the bulk resistivity and optical transmission at two microns wavelength of SnO_2 films doped with antimony and other materials. Their results showed strong minima in both these properties occurred with antimony doping of about three

percent by molar content.

Indium, when included in the n-type semiconducting SnO_2 , acts as an acceptor. The addition of In^{3+} ions neutralizes defect center O^{2-} deficiencies.⁽²⁾ The indium atoms, like antimony, substitute for tin atoms in the crystal structure, giving it the empirical formula of



Studies by A. Rohatgi, et al.,⁽¹³⁾ show that between one and four molar percent indium doping, the bulk resistivity and transmission at two μm . wavelength was increased by several orders of magnitude, while above this percentage there was little change. This suggests that the additional indium present, when basically all the oxygen defects have been neutralized, has no large effect on the properties of the SnO_2 film.

In general, the addition of impurities of the types mentioned act as donors or acceptors in the SnO_2 which is an n-type semiconductor intrinsically. The impurities act by increasing or decreasing the number of conduction electrons in the material. This means that the impurities apparently do not increase the band-gap but rather shift the point of the band-gap transition by filling up the conduction band and thus changing the Fermi level. There are three levels of effect by impurities on the energy band structure. At low densities, discrete localized energy levels are formed in the forbidden band. At medium concentrations, these discrete levels overlap to form a conducting impurity band, still within the forbidden band-gap. At higher concentrations, this impurity band overlaps with the conduction band.⁽⁸⁾ In this

study, only the last case is of interest as the lower concentration effects are not readily observable. The overlapping impurity band creates a density-of-states and absorption edge tail which extends into the forbidden gap. Tails may also be formed by deformations and phonons, but all tails are usually masked by the shift of the absorption edge to higher energies due to the filling of the conduction band with electrons.

CHAPTER 3

EXPERIMENTAL PROCEDURE

3.1 Sample Preparation

The tin dioxide tin films were prepared by spraying a tin chloride solution on one side of heated, optical quality quartz substrates. The substrates, approximately one inch square by one eighth inch thick, were heated to between 800 °C. and 850 °C. over a Bunsen burner.

The basic tin chloride solution consisted of tin chloride, hydrochloric acid, and water with the proportions: 350 ml. of SnCl_4 to 250 ml. concentrated HCl to 108 ml. of H_2O . This solution was sprayed on the heated substrates by itself for the undoped samples and with antimony or indium chlorides added for the doped samples. A ten percent doping level was achieved with antimony by adding 54 ml. of SbCl_5 per liter of the basic solution, and with indium by adding 94 g. of InCl_3 per liter. Doping levels of five, two and one half, and one percent were achieved by mixing proportional amounts of the basic solution and the appropriate ten percent doped solution.

The solutions, as formulated above, were applied with a spray atomizer in an air atmosphere, until a cloudy layer, free of visible interference phenomena, was built up on the surface. The films were approximately ten microns thick, but often were of uneven thickness

and appearance due to the inherent problems of this type of application.

After measurement, an undoped sample was selected for further study. This further study consisted of three stages, after each of which the sample was re-tested. The first stage consisted of ageing for 52 days. The other two stages consisted of re-heating the sample to between 650 °C. and 700 °C., first in a vacuum (10^{-5} Torr.), and in the final stage, in air. These two treatments each lasted about four hours.

3.2 Resistance Measurements

The resistivities of the thin film surfaces were measured using a non-destructive contacting probe. The probe consisted of two parallel strips of copper, each one centimeter long and separated by one centimeter. Thus the probed area was one centimeter square with contacts along two sides. The width of each strip which was in contact with the surface was about two millimeters. To complete the measurement the two contacts were connected to either a V.O.M. or a digital V.T.V.M., both being set to measure resistance. There was no observed difference between the results with the V.O.M. and those with the V.T.V.M.

3.3 Optical Measurements

All the samples were observed optically within a week of being made. Optical measurements were made with a Beckman DK - 2 split beam spectrophotometer equipped with an MgO coated integrating sphere. For transmission measurements the SnO₂ sample and an uncoated substrate were placed in the sample and reference beams respectively.

For reflection measurements, the SnO_2 sample, with a black backing material, and an MgO plate were placed so as to reflect the sample and reference beams respectively into the integrating sphere where light scattered over all angles was collected. Then, the procedure was repeated with the sample removed to measure the reflectance contribution of the backing material.

Over the wavelength range of 0.5 to 2.6 micrometers, a tungsten source and a PbS detector were used. Over the range of 0.2 to 0.6 micrometers, a hydrogen discharge light source and a photo-multiplier tube detector were used. The signal from the detector was integrated with a time constant of four seconds before recording, which limited the resolution of wavelength to approximately $0.013 \mu\text{m}$. above $0.36 \mu\text{m}$., and to approximately $0.0013 \mu\text{m}$. below $0.36 \mu\text{m}$. The transmittance and reflectance were recorded as percentages, and the accuracies of these readings were taken as $\pm 0.5 \%$ for transmittance and $\pm 1.0 \%$ for reflectance. The accuracies of the wavelength measurements were taken as 10^{-8} m . above $0.36 \mu\text{m}$. and 10^{-9} m . below $0.36 \mu\text{m}$.

CHAPTER 4

RESULTS

4.1 Preparation Effects

The effects of the preparation method can be divided into two broad areas, chemical effects (impurities) and physical effects (film thickness, surface condition). The major impurity contributions are chlorine ions and oxygen deficiencies, the theory of which has been discussed in the preceeding chapter. The dependance of these impurity concentrations on such parameters as the temperature and rate of application of the film as well as the film environment have not been satisfactorily investigated to this point and remain an unknown. As these parameters vary slightly from sample to sample, an element of uncertainty is introduced into the investigation. It has been suggested in some studies that films formed at a higher temperature (around 950 °C.) may be more stable in their properties, indicating lower defect concentrations; however, this is not conclusive. Another type of impurity comes not from the reaction solution but from the reaction environment. On occasion, contamination was found both from the gas feeding the Bunsen burner and from the support and protection set up for the substrate. This was mainly constructed of ceramic and firebrick, which tended to crumble under the combination of heat and chemicals. Possible contaminants include small amounts

of hydrocarbons and carbon, iron, nickel, and silicon. The possibility of other contaminants in the air cannot be discounted.

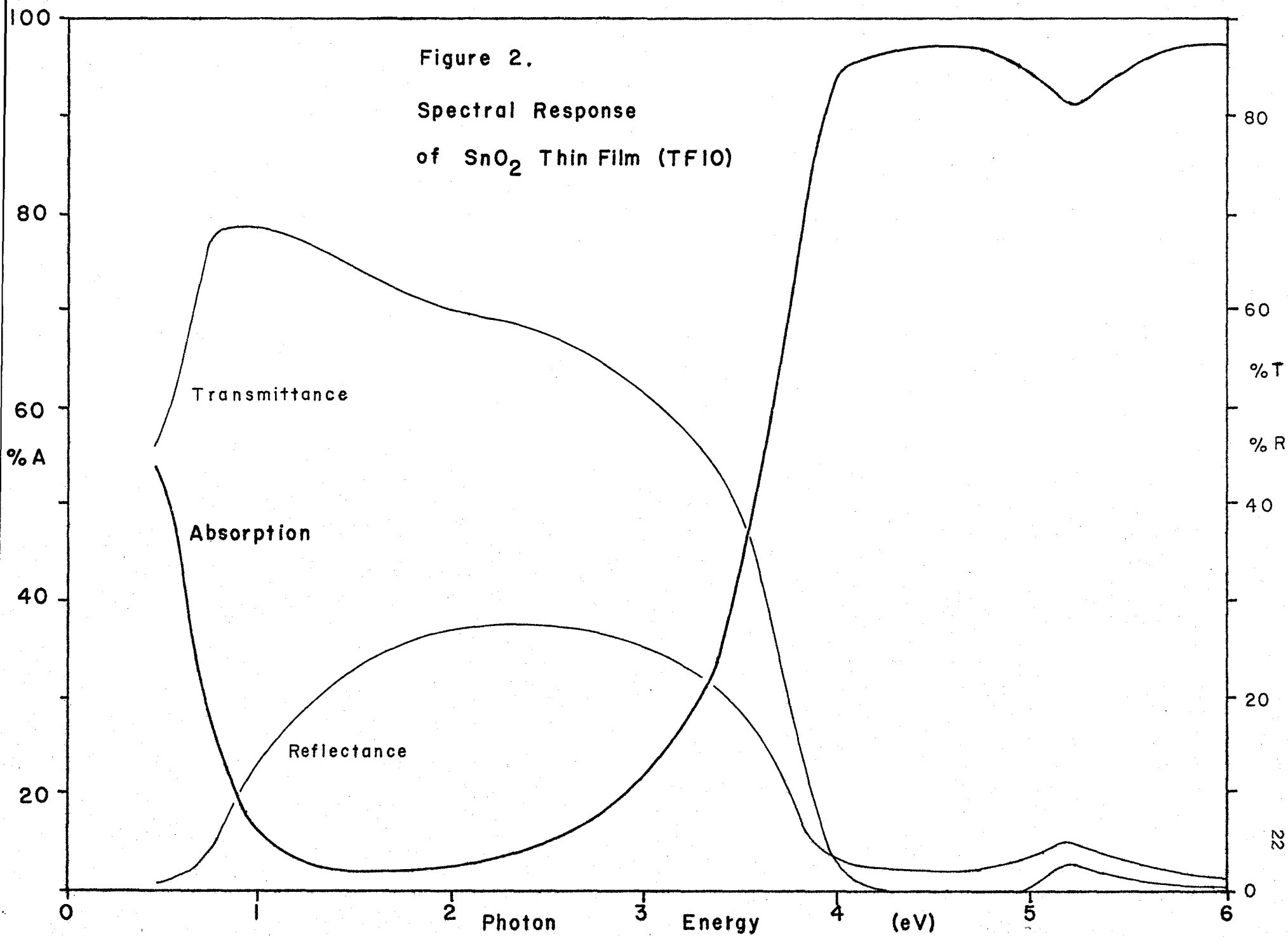
The temperature, rate, and conditions of application with which the films were formed also had a definite effect on the physical properties of the films, such as grain size, surface continuity, and bulk continuity (as indicated by the cloudiness of the film) and uniformity of film thickness. The grain size and film continuity affect the resistance measurements while the thickness and cloudiness of the film mainly affect the optical measurements.

A good example of the effects of the environment on sample characteristics was found in samples 21 and 22. These samples were prepared with a ten percent indium doped solution and using a different support system from the other samples. The main difference in the support system was that it allowed more cross air-circulation to the sides of the substrate during firing. The effect of this increased cross-current activity was large enough that these samples could not be comparatively studied with reference to the other samples. (The effect on these samples can be seen in figure 9.)

Except for the above mentioned two samples, however, all the other samples compared quite well with each other, with literature values, and with theoretical expectations, and showed definite relationships with the parameters being measured. Thus it can be assumed that the data and the relationships formed from this data are representative of the actual case with tin dioxide films of this type.

Figure 2 shows the spectral response of a typical undoped tin dioxide film. The major factor in this response is the area of

Figure 2.
Spectral Response
of SnO_2 Thin Film (TF10)



almost total transmission from 0.5 eV. to 3.5 eV. The lower absorption edge at about 0.5 eV. was found to vary quite dramatically with doping level. The upper absorption edge at about 3.5 eV. was found to vary less dramatically but uniformly with doping. This edge occurs at the band-gap energy as described in chapter 2. The exact position of this edge was found by plotting the absorption coefficient, as is shown for one film in Figure 3, and extrapolating to zero. The film thickness, being unknown, appears as a constant which has no effect on the zero crossing of the absorption coefficient curve and its extrapolations. This curve can also provide information about the phonon energies involved in the band-gap transition. This is why two extrapolations, representing E_g and $E_g + E_p$, are shown in Figure 3. (A third, $E_g - E_p$, is also possible.) An additional factor in the spectral response on SnO_2 is a slight dip in the absorption at 5.2 eV., as seen in Figure 2. The exact cause of this dip is unknown, but it was found to be invariant under all doping and treatment conditions.

The band-gap energies obtained from the absorption coefficient curves ranged from 3.67 eV. to 3.70 eV. for pure SnO_2 which is in good agreement with the values obtained by other researchers.^(1,7) The value for the phonon energy for the SnO_2 band-gap transition was 0.06 to 0.07 eV. which agrees well with the maximum theoretical value of 0.08 eV. for pure SnO_2 .⁽⁴⁾ However, no evidence was found to support the measurements of W. Spence⁽⁷⁾ for direct transition (4.3 eV.), indirect transition (2.7 eV.), and impurity (3.36 eV.) peaks.

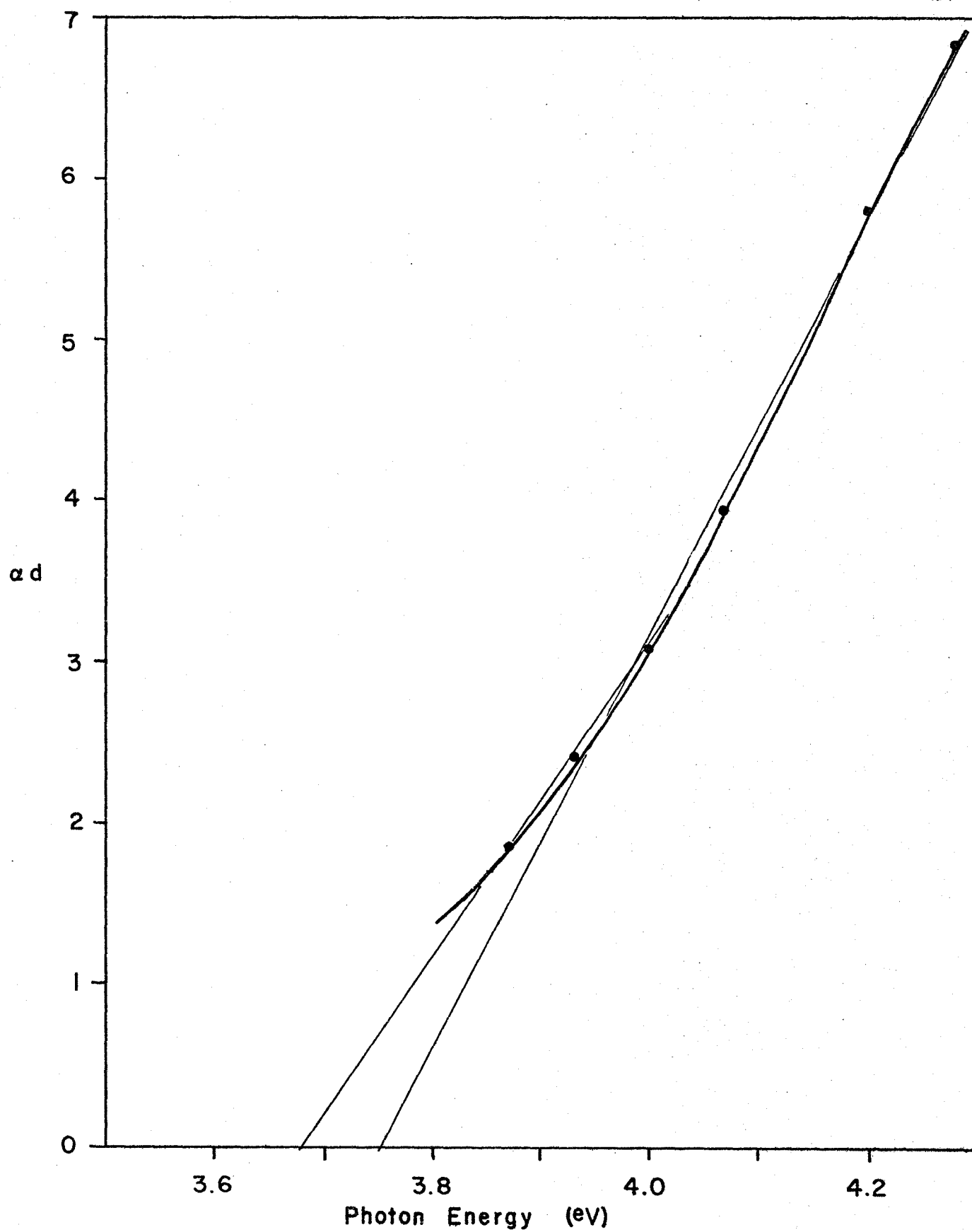


Figure 3.
Absorption Coefficient \times Film Thickness
for SnO_2 (TFI2d)

4.2 Antimony Doping

Antimony doped SnO_2 samples similar to the undoped samples were produced with antimony doping levels of 10 %, 5 %, 2.5 %, and 1 % by molar concentration. All samples had the same cloudy white appearance of the undoped samples; however, the more heavily doped samples displayed a blueish tint, due to absorption in the near infra-red spectrum. This factor is apparent in Figure 4., which compares the spectral response of an antimony doped sample (10 %) with that of an undoped sample. The blueish tint is caused by the large absorption peak at 0.6 eV. which in turn is caused by a large free carrier concentration. As discussed in chapter 2, it is the fact that this free carrier plasma frequency occurs in the near infra-red in conjunction with the high band-gap energy that gives SnO_2 transparency in the visible spectrum.

It can be seen in Figure 4. that the major absorption edge, above 3.7 eV., has been shifted to a higher energy in the antimony doped sample than in the undoped sample. The position of this absorption edge as a function of doping level shifts according to a positively increasing, non-linear function; as plotted in Figure 5. The absorption edge positions were computed both from extrapolations of the absorption coefficient graphs, and by graphing the first derivatives of the absorbance curves to find the point of maximum slope. Of the two methods, the former is the more widely accepted. By this method, the absorption edge for 10 % antimony doped SnO_2 is found to occur at 3.79 eV. as compared with undoped SnO_2 for which the edge is found to occur at 3.68 eV. This higher energy level is made

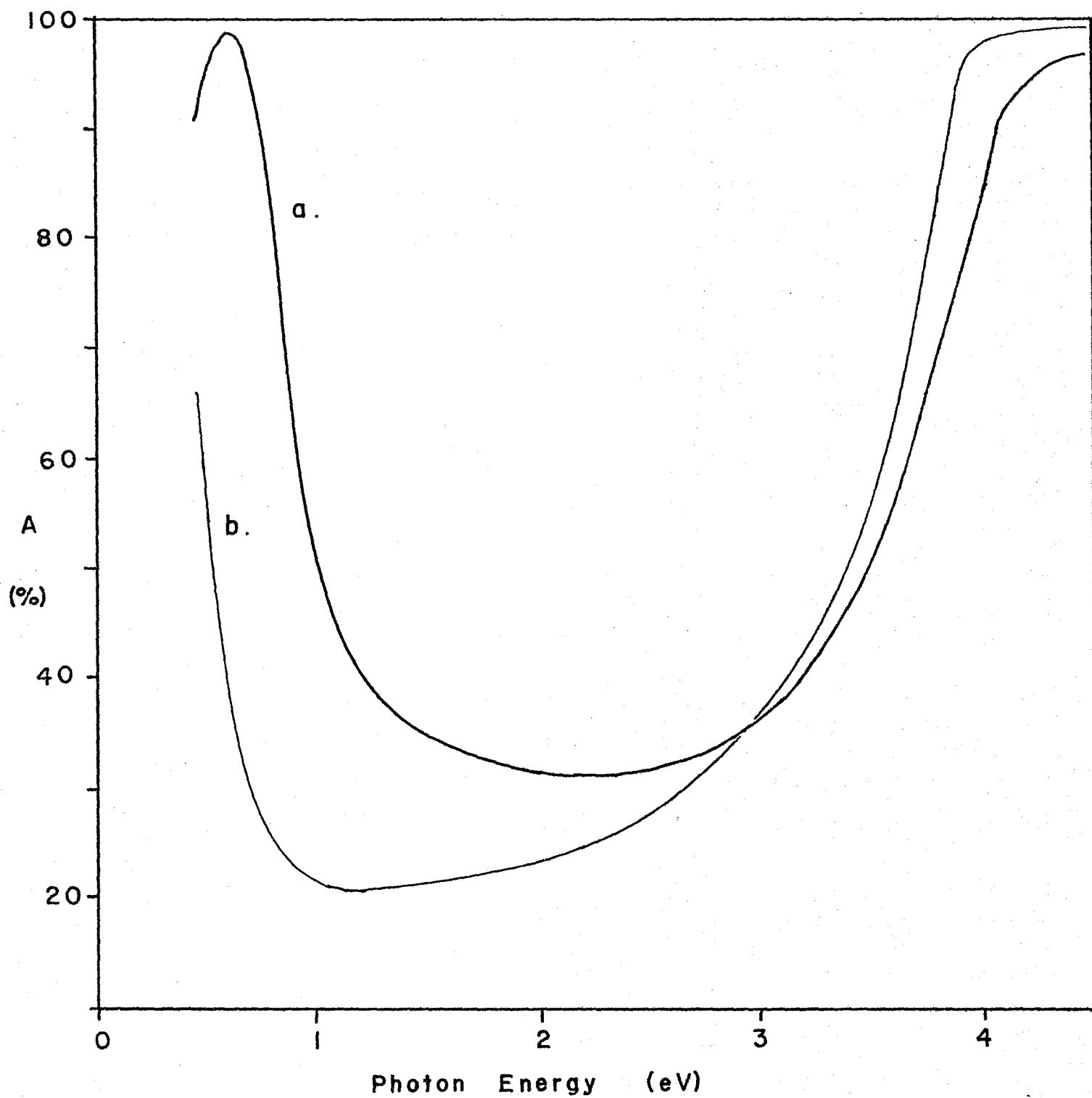


Figure 4.
Absorption Spectra of: a. 10% Sb Doped SnO₂ (TF16)
b. Undoped SnO₂ (TF12a)

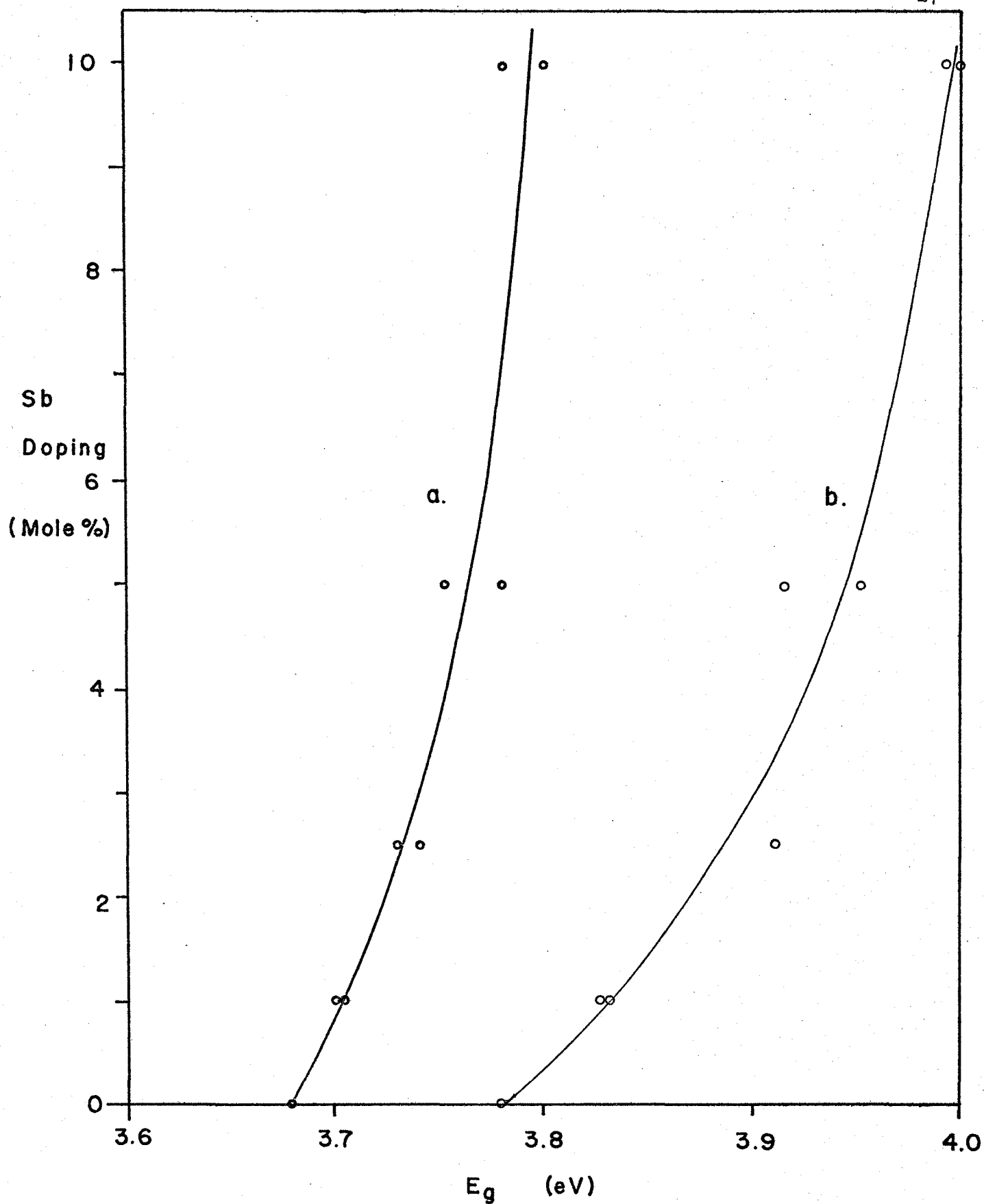


Figure 5.
Absorption Edge Energy of Sb Doped SnO_2
by αd (a) and $dA/d\lambda$ (b.)

up of the band-gap energy for SnO_2 plus an activation energy (as shown in Figure 1.) which also increases as the doping level increases. The higher activation energy is a result of the raising of the Fermi level of the material introducing more free carriers to the conduction band. Thus, as the lower energy levels of the conduction band become more filled up, electrons from the valence band must be excited to a higher energy to reach an unoccupied conduction band level. The increase in energy with doping is not linear, it increases more slowly at higher doping levels. This might tend to suggest a saturation effect, whereby as the doping concentration is increased, the proportionate probability of additional antimony adding to the conduction band is reduced.

The effect of antimony doping on the surface resistivity is to reduce it, as shown in Figure 6, from 4000 ohms for undoped samples to about 40 ohms for samples with a doping level of ten percent. The curve of resistivity versus doping can be divided into two sections, a steeply curving section below the one percent doping level, and a roughly exponential section at higher doping levels. This suggests that possibly there are two mechanisms involved in free carrier generation, depending on the doping level. It is also suggestive of the saturation effect mentioned in the preceding paragraph.

Associated with the increase in photon energy needed for transition to the conduction band due to doping, there is an increase in phonon energy needed as well. This energy increases linearly with increased doping level and is plotted for antimony in Figure 7. The phonon gives the electron involved the energy for the positional change

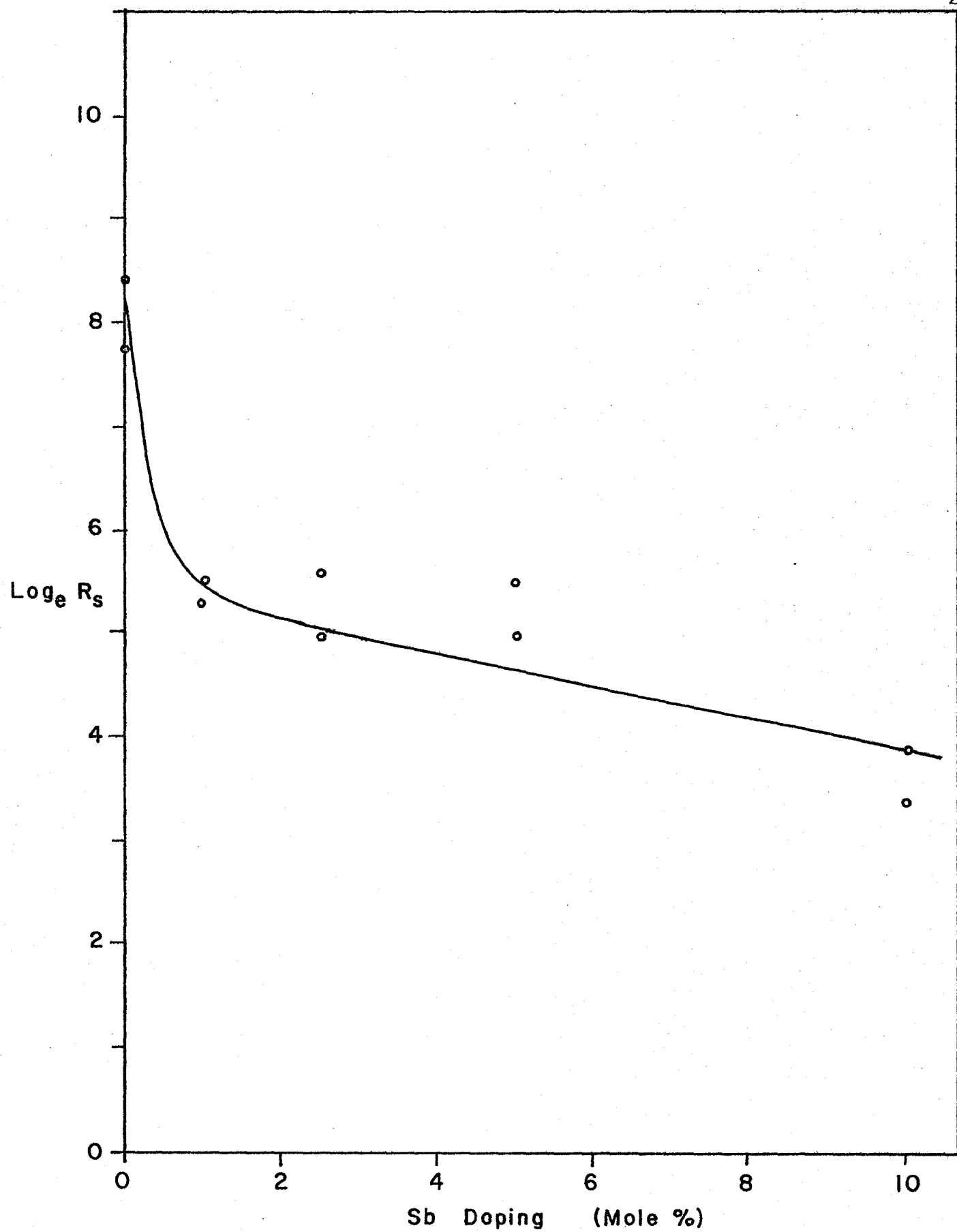


Figure 6.
Surface Resistance per cm^2 of Sb Doped SnO_2

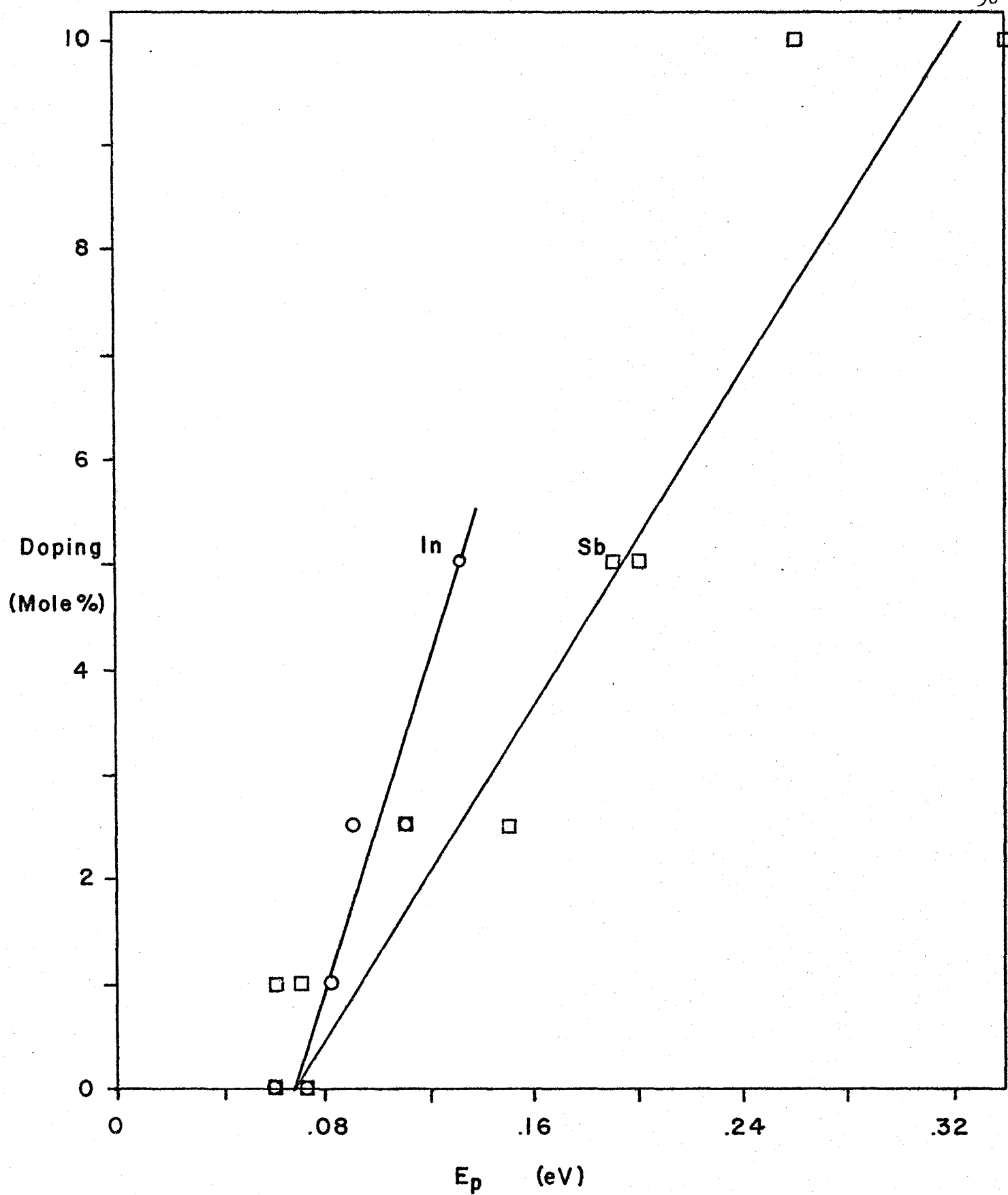


Figure 7.
Phonon Energy for Sb , In Doped SnO₂

necessary for an indirect transition. There are two possible explanations for this increase in the phonon energy needed. First, as more and more energy levels in the conduction band are filled, the point of transition in k-space is pushed further away from the minima in the upper limit of the valence band (see Figure 1) requiring a greater phonon energy. The second possible cause is the effect of antimony on the crystal lattice of tin dioxide. A large doping level could be expected to produce a strain in the lattice, which in turn would require the transition electrons to have a higher phonon energy. It is probable that both these causes contribute to the increase in phonon energy. This energy increases from below 0.08 eV. for undoped SnO_2 (as required by theory) to approximately 0.3 eV. for the 10 % antimony doped samples.

A study by A. Rohatgi, et al.,⁽¹³⁾ reports definite minima in the curves of transmission at two microns wavelength and resistance versus antimony doping. These minima occur at 3 % antimony doping, after which transmission and resistance increase. These curves and their minima are in almost total disagreement with the results of the investigations for this report and are not explained by the theory presented herein.

4.3 Indium Doping

Indium doped SnO_2 samples similar to the undoped and antimony doped samples were produced with indium doping levels of 5 %, 2.5 %, and 1 % by molar concentration. All samples had the cloudy white appearance common to SnO_2 samples in this study. Samples were also

produced with indium doping of ten percent; however, as discussed in section 4.1, these samples were atypical. Their appearance was much the same as the other samples except that the film surfaces were more broken up and non-uniform.

The spectral response of an indium doped (5 %) thin film, as shown in Figure 8 compared with an undoped SnO_2 film, shows an absorption peak at 0.6 eV. but at a very low absorption level. Absorption at this point is due to free carriers in the material, and a low absorption level indicates a low free carrier density.

As with antimony doping, the absorption edge above 3.7 eV. has been shifted to a higher energy in the indium doped sample than in the undoped sample, as can be seen in Figure 8. This increase in absorption edge energy is a function of doping level, as shown in Figure 9, and is very similar to the increase found with antimony doping, although the theoretical explanations for the two effects are widely different. The methods used to compute the absorption edge energies for indium are the same as those used for antimony. Using the absorption coefficients, the absorption edge for 5 % indium doped SnO_2 was located at 3.77 to 3.80 eV., almost identical with the edge location for 10 % antimony doped SnO_2 , and above the edge location for undoped SnO_2 at 3.68 eV. It is not likely that the actual band-gap of SnO_2 is altered appreciably by indium doping. It is more probable that the increased forbidden gap transition energy results from depression of the Fermi level below the upper limit of the valence band, causing the top energy levels of the valence band to be vacant. Thus, excited electrons from the top levels of the valence band that are occupied must possess an

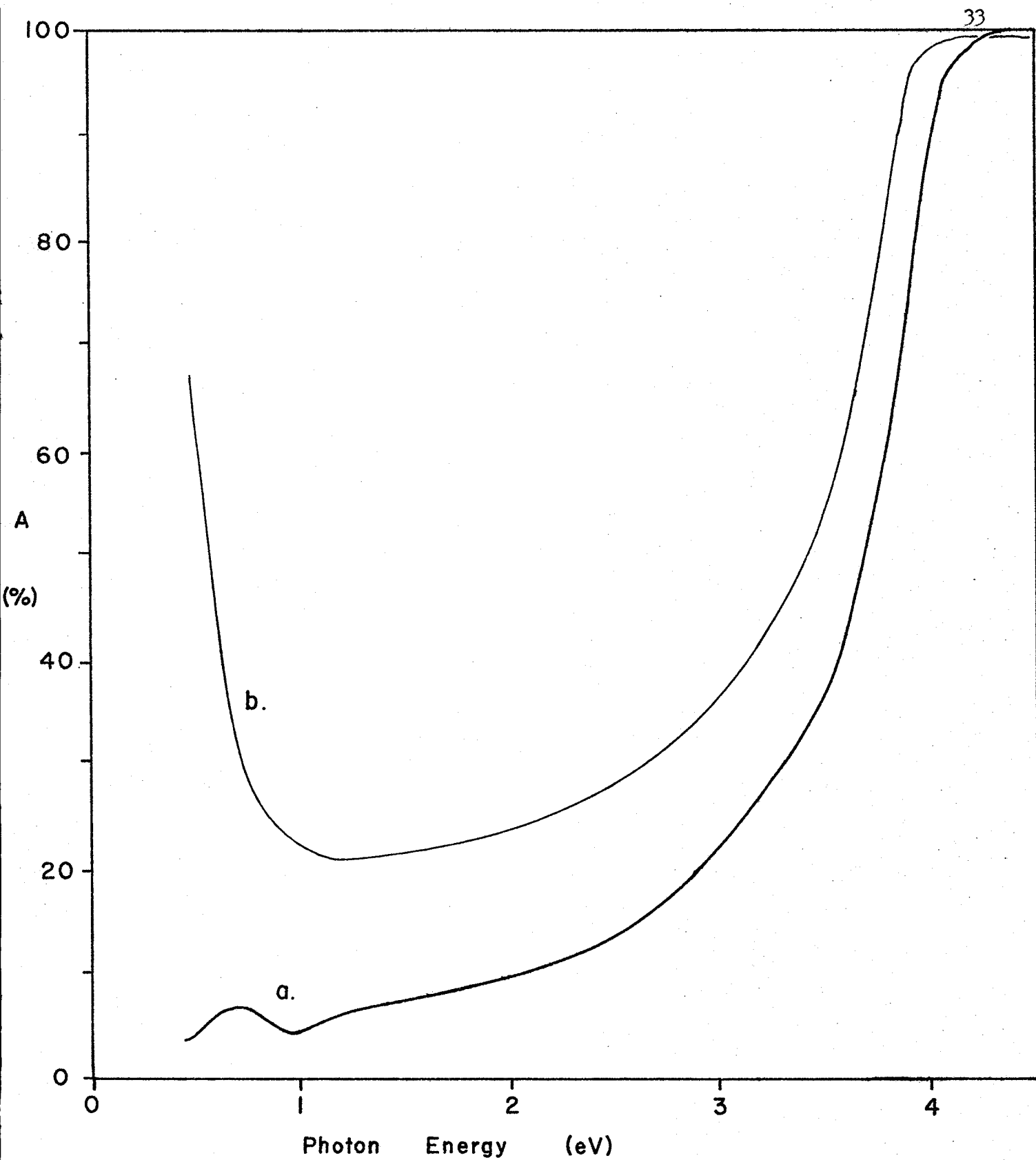


Figure 8.
Absorption Spectra of : a. 5% In Doped SnO₂ (TF 24)
b. Undoped SnO₂ (TF 12a)

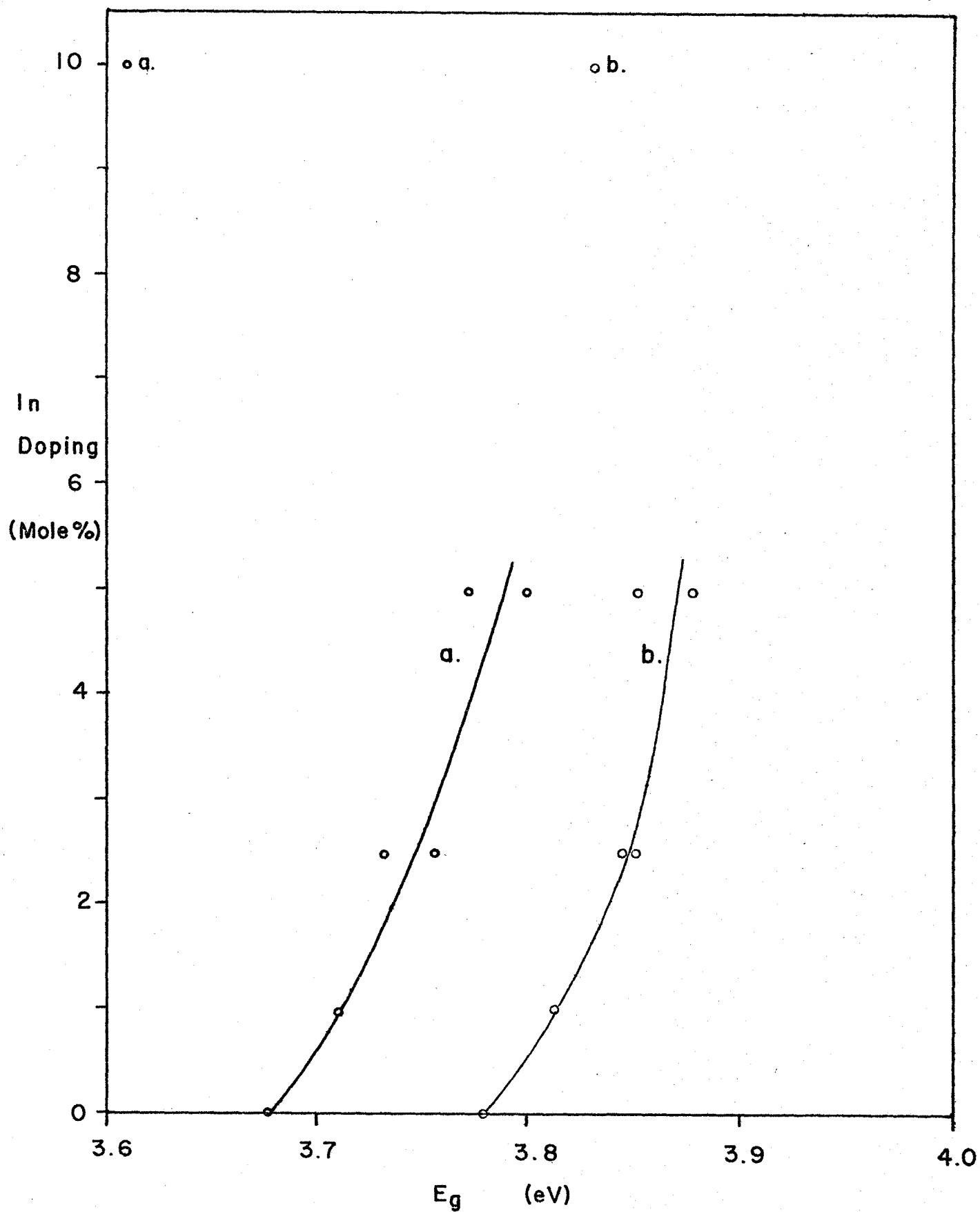


Figure 9. Absorption Edge Energy of In Doped SnO_2 by αd (a.) and $dA/d\lambda$ (b.)

energy equal to the energy of the forbidden gap plus the energy required to reach the top of the valence band from their starting levels. The curve of the energy increase with doping (Figure 9) suggests that as doping level increases, the efficiency of the indium in depressing the Fermi level is decreased. Indium would depress the Fermi level by tying up electrons and thus removing them from the valence and conduction bands of the material.

The effect of indium doping on the surface resistivity of tin dioxide is to increase it, as shown in Figure 10, from 4000 ohms for undoped samples up to 4×10^6 ohms for 5 % indium doped samples and to over 20×10^6 ohms per square for 10 % doping levels. As with antimony doping, the curve of resistivity versus doping can be divided into two regions, a steeply curving section below one percent doping, and an exponential section at higher doping levels. This suggests the involvement of two mechanisms in the free carrier generation as mentioned in section 4.2.

Associated with the increase in band transition energy indicated by the absorption edge is an increase in phonon energy. This phonon energy increases linearly with increased doping level, and is plotted for indium doping, along with antimony doping, in Figure 7. The most probable cause for this increase is the strain introduced into the lattice by the high level of doping, as discussed in section 4.2. As the phonon energy behaves similarly for antimony and for indium, it is probable that the strain is the major cause of the phonon energy increase for antimony as well as for indium. The phonon energy increases to 0.13 eV. for 5 % indium doped SnO_2 from a level of 0.06 to 0.07 eV.

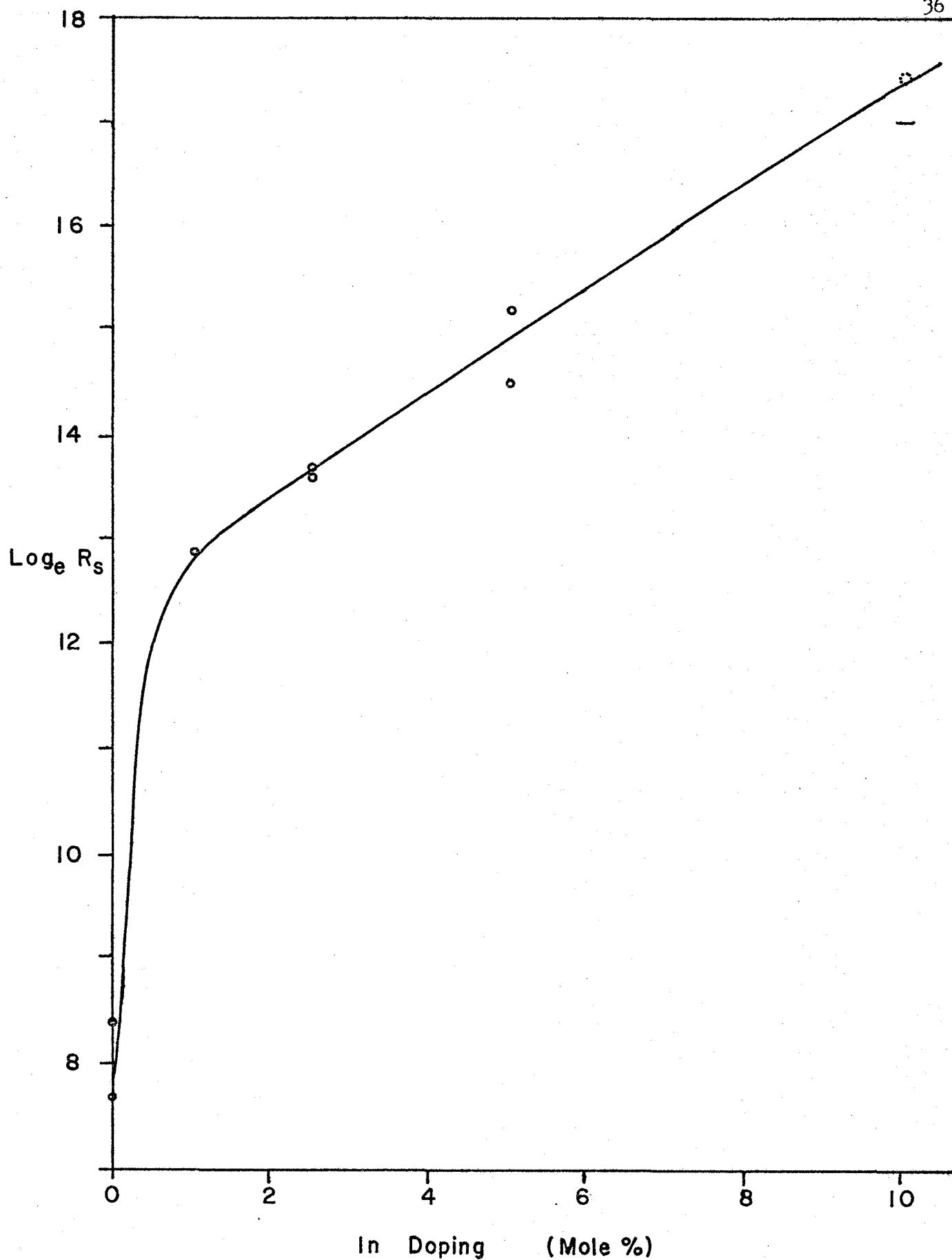


Figure 10. Surface Resistance per cm^2 of In Doped SnO_2

for undoped samples. This is compared with 0.19 to 0.20 eV. for 5 % antimony doped samples.

A. Rohatgi, et al.,⁽¹³⁾ indicate that curves of transmission at two microns wavelength and resistance versus doping flatten out at a doping level of approximately 3 % for indium doped SnO_2 . As with antimony doping in section 4.2, the Rohatgi study and this report do not agree on these points.

4.4 Self-Doping

To study the self-doping effects of tin dioxide, a representative sample of undoped SnO_2 was treated in three ways. First it was aged for 52 days. Second, it was heated to about 660°C . for two hours in a vacuum (10^{-5} Torr.) and then allowed to cool over two hours. The third treatment was to heat the sample, as with the second treatment, except that this treatment took place at room pressure. At each stage in the treatment series, the same measurements were made on this sample as were made on the doped samples. The observed absorption spectra for the four stages are shown in Figure 11. The absorption edge energies computed from these spectra are given in Figure 12, and the surface resistivities for the film under the four situations are plotted in Figure 13.

The main change that took place in the film as it aged was a reduction in the absorbance in the visible window of the SnO_2 spectrum by about 20 percent as seen in Figure 11. If the entire spectrum of the new sample were shifted down by this factor, it would super-impose, within error, over the spectrum of the aged sample, except where both

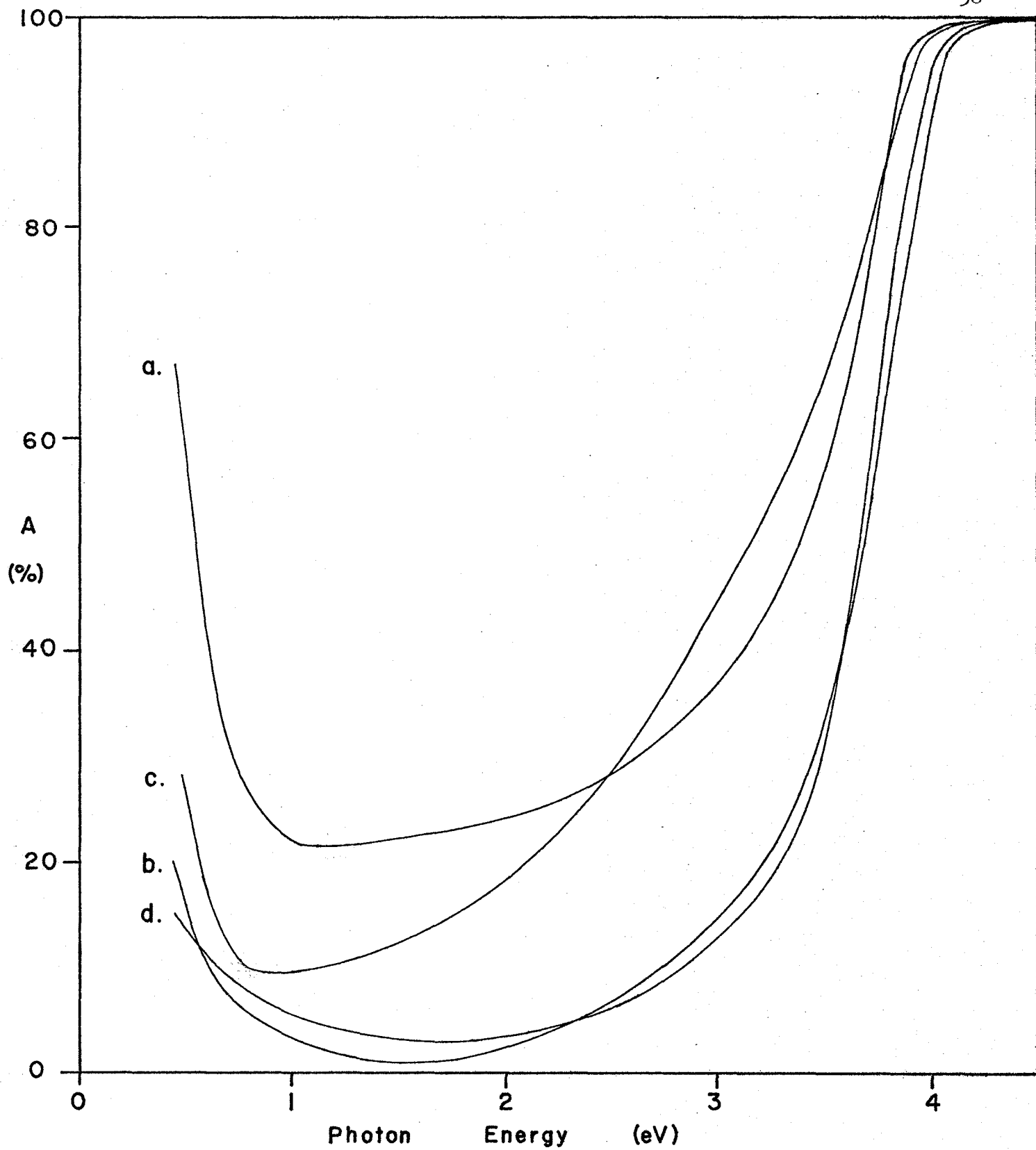


Figure 11. Consecutive Absorption Spectra of SnO₂ (TF12)
a. as made c. vacuum annealed
b. aged d. air "

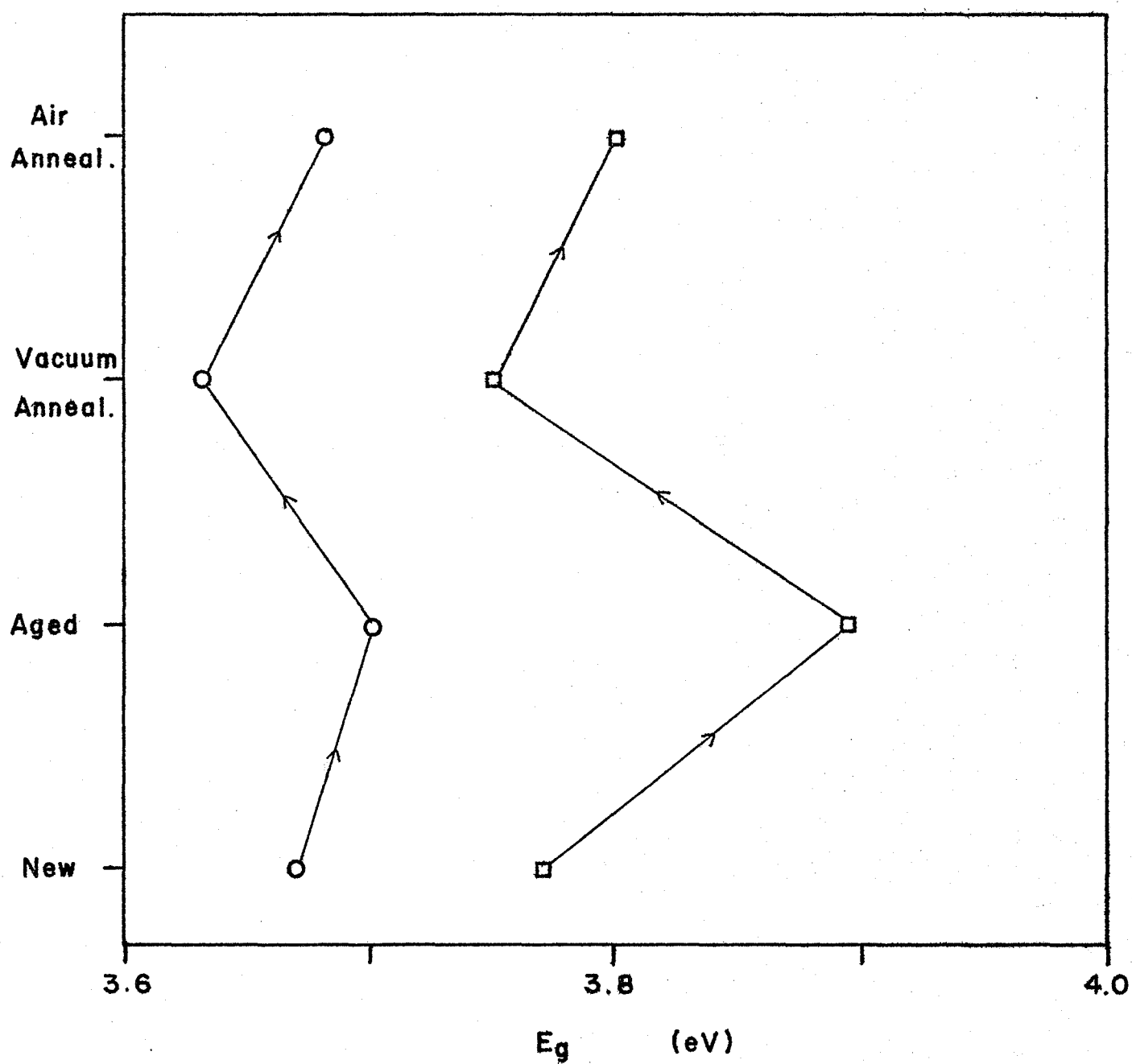


Figure 12.

Absorption Edge Energy of Treated SnO_2
by ad (O) and dA/dλ (□) (TF12)

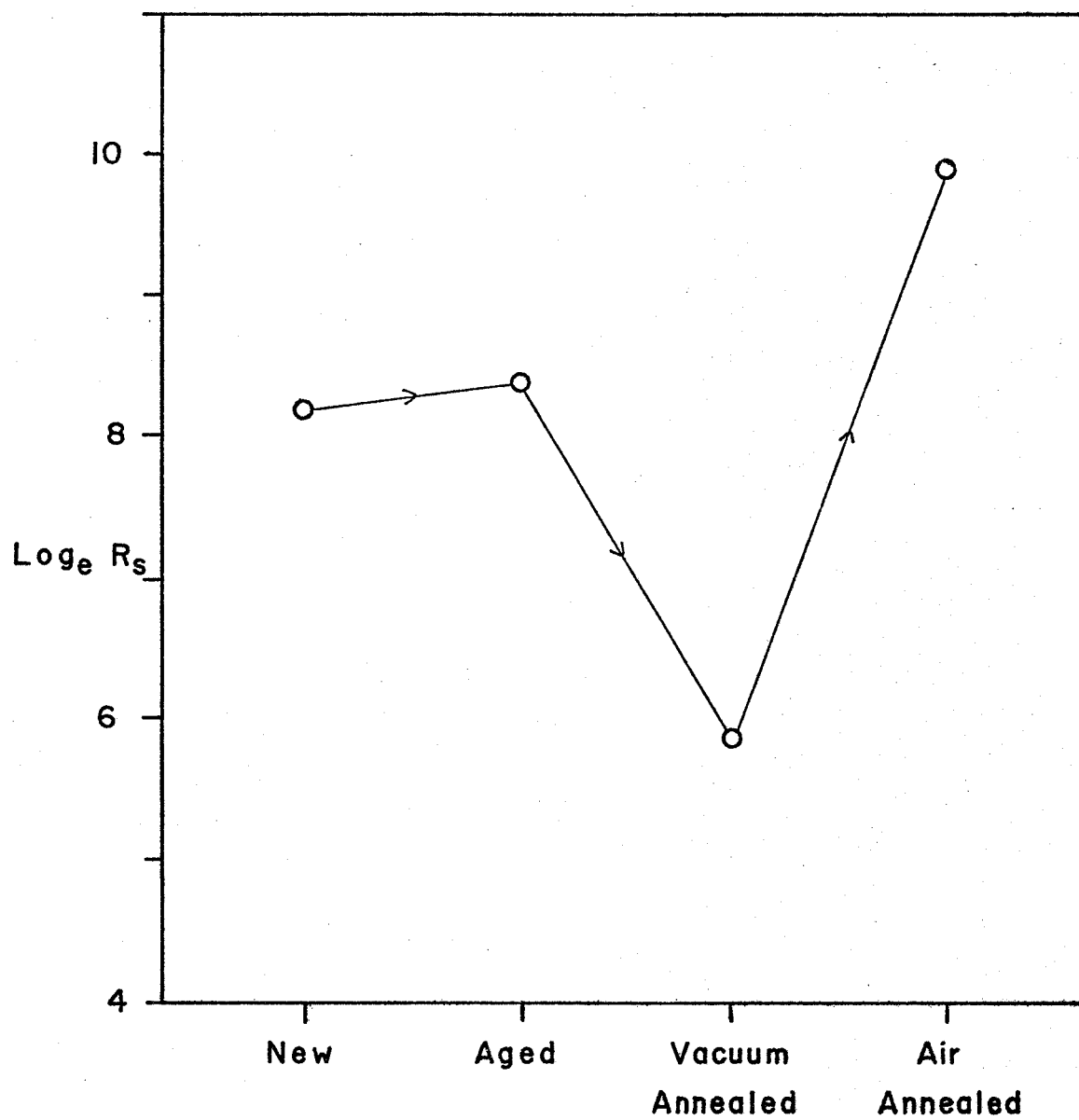


Figure 13.

Surface Resistance per cm^2
of Treated SnO_2 (TF12)

curves go above 80 percent. The absorption edge of the new film was slightly lower than that of the film after aging (3.67 eV. new; 3.70 eV. after aging) but this could be accounted for by shifting the spectrum down by the 20 % difference and by errors in measurement. The unshifted spectra also seem to indicate a higher free carrier concentration in the new film, but almost equal surface resistivities (3800 ohms per square for the new film; 4500 ohms after aging) argue against this. The most satisfactory explanation of the differences after aging is that the film had lost some of its cloudiness with time resulting in less loss due to scattering during transmission measurements. There are two possible causes of this. One cause could be the wearing off of a powdery outer layer of the film, leaving a more solid film below. The other possible cause would have been a natural cohesive reaction in the film resulting in an annealing effect. The first cause is the more probable one.

Heating the film in vacuum had a definite effect on both the absorption edge and the resistance as can be seen in Figures 12 and 13. The absorption edge dropped from 3.70 eV. to 3.63 eV. and the resistance dropped from 4500 ohms to 360 ohms per square. Heating in vacuum should drive off oxygen atoms from the film. These oxygen deficiencies in the SnO_2 structure would result in larger free electron concentrations and therefore higher conduction. The lowering of the absorption edge position could indicate the formation of a defect conduction band within the forbidden band-gap.

Heating the sample in air caused the absorption edge energy to return to 3.68 eV. which can be considered as essentially the value

it had before either heat treatment. As can be seen from Figure 11, the spectra before and after the two treatments are almost identical; however, the surface resistivity of 20,000 ohms was about four times that of the untreated film. Also, the surface of the film had a different appearance, due mainly to a self-cleaning effect which had oxidized away surface dirt. The increased resistance of the surface probably resulted not from a change in free carrier concentration but from a change in surface condition so that the probe did not make as good contact as previously. Or, alternatively, the heat treatment may have introduced cracks into the film. In terms of oxygen deficiencies, the heating in air seems to have completely erased the effects of the vacuum heat treatment.

CHAPTER 5

CONCLUSIONS

The effects of non-uniform film conditions and the possible inclusion of trace contaminants on this study appear to be minimal in spite of the large potential for variation in the method of creation of the tin dioxide thin films. While better preparation conditions would have rendered these results more accurate, the results themselves would not be significantly different.

The antimony doped samples exhibited increased absorption at 0.6 eV. representing increased free carrier absorption. As antimony is expected to act as a donor in SnO_2 , this greater free carrier concentration is consistent with the theoretical picture of the doping condition. Reduced resistivity also confirms the increased free carrier concentration.

Observations of the energies of photons absorbed to elevate electrons from the valence band to the conduction band showed an increase in both the photon energy and the phonon energy needed for this transition. The higher photon energy confirms the theoretical prediction that the increased carrier concentration introduced by the antimony raises the Fermi level, thus filling up the lower conduction band levels and resulting in a higher activation energy. The increased phonon energy is predicted in theory, as the filling up of the lower

conduction band levels should result in a shift in the point of transition. Also, strains on the lattice structure, such as those introduced by antimony, generally result in a shifted phonon energy.

The indium doped samples exhibited reduced absorption at 0.6 eV, indicating reduced free carrier concentration. As indium is expected to act as an acceptor in tin dioxide, this is also consistent with the theoretical description of this situation. The increased resistance exhibited by the samples is another indication of reduced free carrier concentration.

As with antimony doping, so with indium doping, observations of photon energies absorbed by electrons in the transition from valence band to conduction band showed increases in both the photon and phonon energies used for this transition. A probable theoretical scheme resulting in the higher photon energies is the formation of an acceptor band by the indium on top of and perhaps overlapping the valence band. This acceptor band would soak up electrons from the conduction band and then from the upper valence levels. This would depress the Fermi level from the conduction band to below the top of the valence band. The measured energy jump would then be from the Fermi level to the conduction band. The increase in phonon energy is probably a consequence of strain on the lattice which would be caused by the large number of doping ions.

The main effect of aging SnO_2 thin films appears to be a reduction in the scattering losses from the film. Whether this effect is due to a change within the film itself or to an external effect on the surface has not been determined.

Heating an undoped sample in a vacuum should theoretically reduce the film by driving off oxygen ions which would increase the free carrier concentration. This increase was observed along with a reduction in the absorption edge energy which could indicate that the oxygen deficiencies act to create a conduction- type impurity band within the forbidden gap, thus reducing the band-gap energy.

Heating the previously vacuum heated sample in air eliminated the effects of the vacuum heating on the absorption spectra and resulted in a higher surface resistance. The higher resistance was probably due to physical changes in the film surface. Heating in air also resulted in a cleaning action on the film surface.

REFERENCES

1. T. Arai, "The Study of the Optical Properties of Conducting Tin Oxide Films and their Interpretation in Terms of a Tentative Band Scheme", J. of Phys. Soc. of Japan 15, 916 (1960).
2. R. E. Aitchison, "Transparent Semiconducting Oxide Films", Australian J. of Appl. Sc. 5, 10 (1954).
3. I. F. Tigane, "Electron-Microscope Investigation of Conducting SnO₂ Films", Soviet Physics - Solid State 7, 212 (1965).
4. Z. Jarzebski and J. Marton, "Physical Properties of SnO₂ Materials", J. Electrochem. Soc. 123, 119c, 299c, 333c (1976).
5. K. Ishiguro, T. Sasaki, T. Arai, and I. Imai, "Optical and Electrical Properties of Tin Dioxide Films", J. of Phys. Soc. of Japan 13, 296 (1958).
6. E. Kanai, Report of Asahi Glass Co. V no. 1, 60 (1955), (in Japanese).
7. W. Spence, "The uv Absorption Edge of Tin Oxide Thin Films", J. of Appl. Phys. 38, 3767 (1967).
8. Moss, Burrell, and Ellis, "Semiconductor Opto-Electronics", Wiley and Sons, New York, 1973.
9. H. Y. Fan, Repts. Prog. Phys. 19, 107 (1956).

10. A. Kahan, "On Determination of Absorption and Reflection Coefficients", Appl. Opt. 3, 314 (1964).
11. V. K. Miloslavskii, "Infrared Absorption of Thin Films of Tin Dioxide", Opt. Spectrosc. 7, 154 (1959).
12. M. Nagasawa and S. Shionya; "Electrical and Optical Properties of Reduced SnO_2 Crystals", p472, and "Electrical and Optical Properties of Oxidized SnO_2 Crystals", p727, Jap. J. of Appl. Phys. 10, (1971).
13. A. Rohatgi, T. Viverito, and L. Slack, J. Am. Ceramic Soc. 57, no. 6, 278 (1974).